

Accepted by Ap. J. Letters

On the Vertical Structure of Radiation-Dominated Accretion Disks

N. J. Turner¹

Physics Department, University of California, Santa Barbara CA 93106, USA

ABSTRACT

The vertical structure of black hole accretion disks in which radiation dominates the total pressure is investigated using a three-dimensional radiation-MHD calculation. The domain is a small patch of disk centered 100 Schwarzschild radii from a black hole of $10^8 M_\odot$, and the stratified shearing-box approximation is used. Magneto-rotational instability converts gravitational energy to turbulent magnetic and kinetic energy. The gas is heated by magnetic dissipation and by radiation damping of the turbulence, and cooled by diffusion and advection of radiation through the vertical boundaries. The resulting structure differs in several fundamental ways from the standard Shakura-Sunyaev picture. The disk consists of three layers. At the midplane, the density is large, and the magnetic pressure and total accretion stress are less than the gas pressure. In lower-density surface layers that are optically thick, the magnetic pressure and stress are greater than the gas pressure but less than the radiation pressure. Horizontal density variations in the surface layers exceed an order of magnitude. Magnetic fields in the regions of greatest stress are buoyant, and dissipate as they rise, so the heating rate declines more slowly with height than the stress. Much of the dissipation occurs at low column depth, and the interior is cooler and less radiation-dominated than in the Shakura-Sunyaev model with the same surface mass density and flux. The mean structure is convectively stable.

Subject headings: accretion, accretion disks — instabilities — MHD — radiative transfer

¹neal.turner@jpl.nasa.gov

1. INTRODUCTION

Black holes in X-ray binary star systems and active galactic nuclei accrete material through surrounding disks of gas. When the accretion rate is greater than about 1% of the Eddington value, the radiation pressure in the central regions of the disk may exceed the gas pressure (Shakura & Sunyaev 1973). The disk structure and the radiation emerging are governed by removal of angular momentum from the gas, and conversion of released gravitational energy to photons. In the standard model, the angular momentum transfer and dissipation processes are unspecified. Both are assumed to occur at rates proportional to the height-integrated total pressure, and the heating is balanced by diffusion of photons to the disk surfaces (Shakura & Sunyaev 1973). The model is unstable to perturbations in mass accretion rate (Lightman & Eardley 1974) and heating rate (Shakura & Sunyaev 1976), and to vertical convective displacements (Bisnovatyi-Kogan & Blinnikov 1977). Any one of these instabilities might substantially modify the disk structure. However, if the stresses are magnetic in nature, buoyancy of the fields may lead to stresses scaling with the gas pressure alone, rather than the total pressure (Sakimoto & Coroniti 1989). In this case the viscous and thermal instabilities are absent. The instabilities may also be eliminated if part of the accretion energy is dissipated outside the disk, in a hot corona (Svensson & Zdziarski 1994). Observed properties that are not understood using the standard Shakura-Sunyaev model include the X-ray emission (Elvis et al. 1978) and UV-optical spectra (Blaes 2004) of active galactic nuclei, and the steady disk luminosities of some stellar-mass black hole X-ray binary systems accreting at 1% to 50% of the Eddington rate (Gierliński & Done 2004).

The most likely physical mechanism of angular momentum transfer in radiation-dominated disks is magnetic stresses. The magneto-rotational instability or MRI (Balbus & Hawley 1991) leads to turbulence in which the energy of differential orbital motion is converted to magnetic fields and gas motions (Hawley, Gammie, & Balbus 1996). In isothermal MHD simulations in which heating and cooling are assumed to balance, magnetic fields generated in the turbulence are partly expelled to form magnetized coronae above and below the disk (Miller & Stone 2000).

Disk structure may be affected also by the locations and rates of heating and cooling. Candidate physical heating mechanisms include resistive dissipation of magnetic fields, microscopic viscous dissipation of gas motions, and radiative damping of compressible turbulence (Agol & Krolik 1998). Cooling processes may include radiation diffusion, convection (Agol et al. 2001), and photon bubble instability (Gammie 1998). Here I examine the effects of heating and cooling on the vertical structure of radiation-dominated disks, using a radiation-MHD simulation.

2. DOMAIN AND METHODS

The domain is a small patch of disk, centered 100 Schwarzschild radii $R_S = 2GM/c^2$ out from a black hole of $M = 10^8 M_\odot$, and co-rotating at the central Keplerian orbital frequency Ω_0 . The local shearing-box approximation is used, and Cartesian coordinates (x, y, z) correspond to distance from the origin along the radial, orbital, and vertical directions, respectively (Hawley, Gammie, & Balbus 1995). The domain extends $1.5R_S$ along the radial direction, $6R_S$ along the orbit, and $6R_S$ either side of the midplane, and is divided into $32 \times 64 \times 256$ zones.

The equations solved and numerical method differ from Turner et al. (2003) in including the vertical component of the gravity of the black hole by a term $-\rho\Omega_0^2z$ in the equation of motion. No viscosity of the Shakura-Sunyaev type is used. The frequency-averaged equations of radiation MHD (Mihalas & Mihalas 1984; Stone, Mihalas, & Norman 1992) are integrated in the flux-limited diffusion (FLD) approximation (Levermore & Pomraning 1981), using the Zeus code (Stone & Norman 1992a,b) with its FLD module (Turner & Stone 2001). Opacities due to electron scattering and free-free processes are included. The equations are closed with a $\gamma = 5/3$ ideal-gas equation of state.

Several dissipation mechanisms may act. A total energy scheme is used during the magnetic field update, so that numerical losses of magnetic field are captured as gas heat. The gas internal energy may also increase through shock compression and associated artificial viscosity. The radiation energy increases when photons diffuse from compressed regions, irreversibly extracting part of the work done in compression (Agol & Krolik 1998; Turner, Stone, & Sano 2002). Gas and radiation remain near mutual thermal equilibrium while heating, owing to free-free absorption and emission. For a steady state, the total dissipation must be balanced by diffusion of radiation, and advection of gas, radiation, and magnetic energy through the vertical boundaries.

The azimuthal boundaries are periodic, the radial boundaries shearing-periodic, and the vertical boundaries allow outflow but no inflow. The radiation flux into each vertical boundary zone is set equal to that between the two adjacent active zones, except that the flux is fixed at zero if needed to prevent radiation energy from entering the domain. Updated boundary fluxes are estimated using photon diffusion coefficients from the previous timestep. A density floor is applied throughout. In zones where the density falls below 0.2% of the initial midplane value, mass is added to bring the density up to the floor level. The corresponding minimum optical depth per zone in the vertical direction is 24.

3. INITIAL STATE

The surface mass density in the calculation sets the total optical depth, and varies from its initial value only through outflows and the density floor. The net vertical magnetic flux affects the accretion stress (Hawley, Gammie, & Balbus 1995), and is time-constant in the shearing-box approximation. Other aspects of the initial condition likely have little effect on the outcome, since the structure is to be determined by accretion stresses, dissipation, and cooling.

The initial condition is a Shakura & Sunyaev (1973) model accreting at 10% of the Eddington value for luminous efficiency 0.1. In constructing the initial state only, the ratio α of stress to total pressure is set to 0.01. The resulting surface density is $1.1 \times 10^6 \text{ g cm}^{-2}$. The half-thickness H of the Shakura-Sunyaev model is $\frac{3}{4}R_S$. The domain outside the model is filled with an ambient medium of the floor density. Since gravity increases with height, while radiation flux is independent of height outside the Shakura-Sunyaev model, the ambient medium is out of hydrostatic balance and falls towards the midplane when the calculation starts.

The magnetic field is given zero net vertical flux, so that outflows can completely demagnetize the domain. The starting configuration is an azimuthal flux tube of circular cross-section, with radius $0.75H$. The axis is offset from domain center by $+0.1H$ in x and $+0.1H$ in z . Field strength in the tube is uniform at 2660 Gauss, corresponding to 4% of initial midplane gas plus radiation pressure. The tube is twisted about its axis, giving maximum poloidal component 661 Gauss. The maximum vertical MRI wavelength of 8 grid zones is adequately resolved. The domain-mean radial field is zero, and the mean azimuthal field of 159 Gauss is much less than values that develop later. The calculation is begun with a small random poloidal velocity in each grid zone. The maximum amplitude of each velocity component is 1% of the midplane radiation sound speed.

4. RESULTS

During the first two orbital periods, the flux tube is stretched radially by MRI, and its upper parts are lifted to the surface of the Shakura-Sunyaev model by magnetic buoyancy. By four orbits, the tube is torn apart by MRI and spread throughout the region within R_S of the midplane. Gravitational energy is released faster than assumed in the initial Shakura-Sunyaev model, and the magnetized region expands into the ambient medium. After 13 orbits, magnetic fields are found throughout the domain.

4.1. Three Layers

The horizontally-averaged structure present from 13 orbits on may be divided into three layers (Figure 1). In a dense layer within about $1.5R_S$ of the midplane, mean magnetic pressure and total accretion stress are less than gas pressure. In lower-density surface layers, magnetic pressure and accretion stress are greater than gas pressure, but less than the sum of gas and radiation pressures. The average structure is marginally convectively stable in the midplane layer. In the surface layers, the gas and radiation Brunt-Väisälä frequencies are about equal to the orbital frequency Ω_0 , and are real, indicating hydrodynamic convective stability.

Magnetic energy is produced fastest near the heights of greatest accretion stress. The fields are buoyant and rise towards the boundaries (Figure 2). The rise speed is approximately the Alfvén speed, as expected for magnetized regions exchanging heat rapidly with their surroundings (Parker 1975). The fields dissipate numerically while rising, and the mean flux of magnetic energy through the boundaries between 15 and 45 orbits is 6% of the mean radiative flux. The horizontally-averaged magnetic pressure is dominated by the azimuthal component throughout, and in most cases the sign of the azimuthal field alternates between consecutive rising regions. The regular pattern seen in figure 2, repeating about every 7 orbits, may result in part from the limited domain size. Rising regions in most cases fill the horizontal extent of the box. In real disks, adjacent buoyant regions may interact.

The photons may partly decouple from the turbulence, in radiation-supported disks accreting via MRI, as the distance radiation diffuses per orbit is about equal to the vertical MRI wavelength (Turner et al. 2003). Large density variations accompany loss of radiation pressure support if magnetic pressure exceeds gas pressure (Turner, Stone, & Sano 2002). The results of the present calculation are consistent with this picture. Density variations on horizontal $x - y$ planes exceed an order of magnitude near the upper and lower boundaries, where the radiation diffusion distance is half the RMS vertical MRI wavelength, and the mean magnetic pressure is more than 30 times the gas pressure. By contrast, horizontal density variations within R_S of the midplane are only a factor two. The average diffusion distance is equal to the RMS vertical MRI wavelength, but the mean magnetic pressure is less than the gas pressure, so magnetic forces squeeze the gas less. At the height $3.3R_S$ where vertical magnetic pressure peaks, the diffusion length is 0.3 times the vertical MRI scale. Although radiation is better-coupled to gas motions, the magnetic pressure is greater than the gas pressure. Density variations are intermediate between those at midplane and boundaries.

The vertical variation in magnetic field strength may be related also to the diffusion of photons through the turbulence. Linear MRI grows slowly if magnetic pressure exceeds

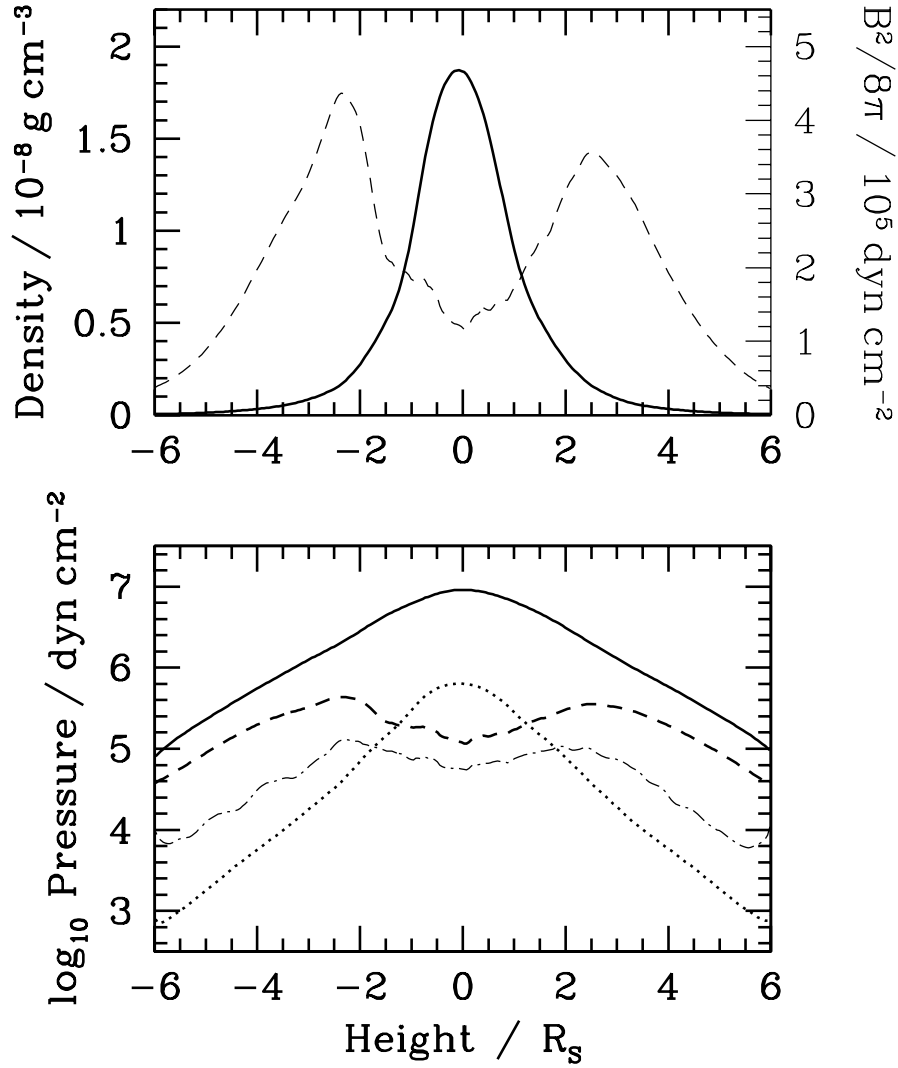


Fig. 1.— Simulation results averaged horizontally and over time from 15 to 45 orbits. The three layers may be seen at top. Curves show density (solid, left scale) and magnetic pressure (dashed, right scale) versus height. The surface layers are optically thick. The optical depth between each magnetic pressure peak and the nearby boundary is 1.5×10^4 . At bottom are plotted the pressures due to radiation (solid), gas (dotted) and magnetic fields (dashed), and the total accretion stress (dot-dashed).

the pressure resisting compression (Blaes & Balbus 1994; Blaes & Socrates 2001). Near the midplane in the simulation, where fluctuations are due largely to the competition of magnetic with gas pressure forces, the turbulence saturates with magnetic pressure less than gas pressure. Around $3.3R_S$, where squeezing is resisted by both radiation and gas pressures, the magnetic pressure is greater than the gas pressure. Near the vertical boundaries, the rate of arrival of magnetic fields from the interior exceeds the local rate of field generation.

The vertical magnetic pressure profile is similar to those in isothermal MHD simulations of gas-supported disks by Miller & Stone (2000). However the magnetized surface layers here are optically thick, and lie inside the disk photosphere. Horizontally-averaged magnetic pressure is everywhere less than gas plus radiation pressure. The total accretion stress at the midplane is half the maximum in the surface layers, whereas in the Miller & Stone (2000) fiducial calculation, total stress in the gas-dominated region varies irregularly with height.

4.2. Comparison with Shakura-Sunyaev Model

The averaged simulation results may be compared against the Shakura-Sunyaev model with the same surface density and radiation flux. The model has $\alpha = 0.0013$ and accretion rate 64% of the Eddington value. Density is almost independent of height in the model interior, while in the simulation the density is centrally-concentrated (Figure 3). In the Shakura-Sunyaev picture, it is often assumed that dissipation is locally proportional to density. By contrast, much of the dissipation in the simulation occurs in regions of low density. Photons escape easily from the surface layers, so the interior is cooler than in the Shakura-Sunyaev model. The midplane ratio of radiation to gas pressure is 160 in the model, and 14 in the simulation. The thermal time in the Shakura-Sunyaev model is 370 orbits, while in the simulation the cooling time, or ratio of total energy content to cooling rate, is just 19 orbits. Dissipation falls off more slowly with height than the stress, as fields tend to rise between generation and dissipation.

4.3. Thermal Balance

The radiation content of the flow is maintained through accretion. Between 15 and 45 orbits, the energy released is 157% of the mean domain-integrated total energy, while the total energy is almost constant, increasing just 2%. The source of power, the differential rotation, is transformed into turbulent magnetic and kinetic energy by magnetic stresses. The turbulence is converted to heat mainly through numerical losses of magnetic fields.

Radiation damping contributes 29% of the heating within R_S of the midplane, where it is readily distinguished from expansion associated with magnetic buoyancy. Artificial viscous heating, mostly in shocks, makes up 12% of the overall dissipation. The dissipation is approximately balanced by cooling. The main cooling processes are diffusion and advection of radiation through the vertical boundaries, with diffusion carrying two-thirds of the energy flux. Mass lost through the boundaries is balanced by mass added to maintain densities above the floor, and total mass increases by less than 1% from 15 to 45 orbits. The energy flux is 73% of the energy input, and the remainder disappears partly through numerical losses of kinetic energy. A complete energy-conserving scheme may be useful for future calculations.

Starting at 50 orbits, the disk heats, then cools. Total energy increases roughly linearly by a factor 2.5 up to 90 orbits, decreases linearly until 145 orbits, then is again steady. The run ends at 170 orbits, or 8 simulation thermal times after first saturation. The heating rate varies, while the diffusion cooling rate is approximately time-constant. No exponentially-growing thermal instability is seen. However, during the hot period, the disk expands, and losses through the vertical boundaries reduce the mass by almost half. The absence of runaway heating may be due to the mass loss, rather than internal thermal stability.

5. CONCLUSIONS

A patch of radiation-dominated accretion disk lying 100 Schwarzschild radii from a $10^8 M_\odot$ black hole is simulated including physical processes of energy release, dissipation, and cooling. The patch has surface density 10^6 g cm^{-2} , and its net vertical magnetic flux is zero. The structure that develops has density greatest at the midplane, stresses greatest in optically-thick surface layers, and dissipation found throughout but intermittent in time and space. The stresses result from magnetic forces. The fields in the surface layers are buoyant. Heating occurs mainly by numerical dissipation of the fields, and physical radiation damping of the turbulence, while cooling occurs by diffusion and advection of radiation through the boundaries. The vertical structure may prove to vary with mass of the central body, location in the disk, surface density, and magnetic flux.

The time-averaged structure in the simulation is hydrodynamically convectively stable. Thermal instability may be prevented by outflow through the boundaries. Viscous stability is not tested, as there is no net radial flow in the shearing box. Photon bubble instability may be present. The fastest linear modes (Blaes & Socrates 2003) in the time-averaged structure are found in the surface layers, have wavelengths shorter than the vertical grid spacing, and grow at $0.9\Omega_0$. Resolved modes, with wavelengths greater than six grid zones,

are expected to grow more slowly than the MRI. No clear signs of these modes are found. The likely direct effect of photon bubbles is to further reduce the cooling time.

The methods used here were developed with Jim Stone and Takayoshi Sano. I benefited also from discussions with Julian Krolik and Omer Blaes. The work was supported by the U. S. National Science Foundation under grant AST-0307657.

REFERENCES

Agol, E., & Krolik, J. 1998, *ApJ*, 507, 304

Agol, E., Krolik, J., Turner N. J., & Stone, J. M. 2001, *ApJ*, 558, 543

Balbus, S. A., & Hawley, J. F. 1991, *ApJ*, 376, 214

Bisnovatyi-Kogan G. S. & Blinnikov S. I. 1977, *A&A*, 59, 111

Blaes, O. 2004, in AGN Physics with the Sloan Digital Sky Survey, ASP Conference Series, G. T. Richards & P. B. Hall, eds., in press

Blaes, O. M., & Balbus, S. A. 1994, *ApJ*, 421, 163

Blaes, O. M., & Socrates, A. 2001, *ApJ*, 553, 987

Blaes, O. M., & Socrates, A. 2003, *ApJ*, 596, 509

Elvis, M., Maccacaro, T., Wilson, A. S., Ward, M. J., Penston, M. V., Fosbury, R. A. E., & Perola, G. C. 1978, *MNRAS*, 183, 129

Gierliński, M. & Done, C. 2004, *MNRAS*, 347, 885

Gammie, C. F. 1998, *MNRAS*, 297, 929

Hawley, J. F., Gammie, C. F., & Balbus, S. A. 1995, *ApJ*, 440, 742

Hawley, J. F., Gammie, C. F., & Balbus, S. A. 1996, *ApJ*, 464, 690

Levermore C. D., & Pomraning G. C. 1981, *ApJ*, 248, 321

Lightman A. P., & Eardley D. M. 1974, *ApJ*, 187, L1

Mihalas, D., & Mihalas, B. W. 1984, Foundations of Radiation Hydrodynamics (Oxford: Oxford Univ. Press)

Miller, K. A., & Stone, J. M. 2000, *ApJ*, 534, 398

Parker, E. N. 1975, *ApJ*, 198, 205

Sakimoto, P. J. & Coroniti, F. V. 1989, *ApJ*, 342, 49

Shakura, N. I., & Sunyaev, R. A. 1973, *A&A*, 24, 337

Shakura, N. I., & Sunyaev, R. A. 1976, *MNRAS*, 175, 613

Stone, J. M., & Norman, M. L. 1992a, *ApJS*, 80, 753

Stone, J. M., & Norman, M. L. 1992b, *ApJS*, 80, 791

Stone, J. M., Mihalas, D., & Norman, M. L. 1992, *ApJS*, 80, 819

Svensson, R., & Zdziarski, A. A. 1994, *ApJ*, 436, 599

Turner, N. J., & Stone, J. M. 2001, *ApJS*, 135, 95

Turner, N. J., Stone, J. M., Krolik, J. H., & Sano T. 2003, *ApJ*, 593, 992

Turner, N. J., Stone, J. M., & Sano T. 2002, *ApJ*, 566, 148

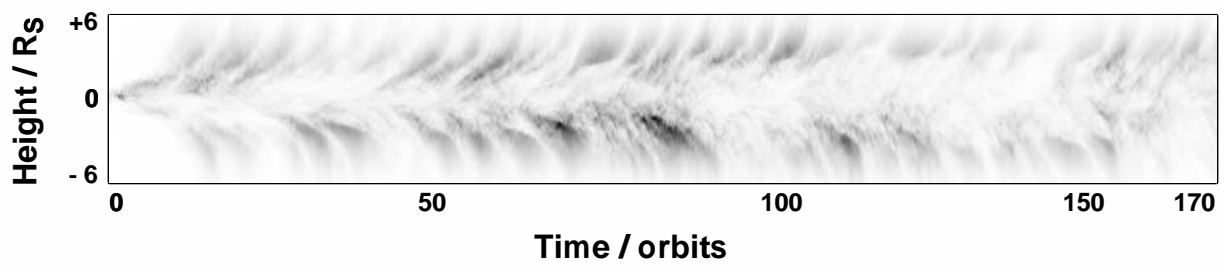


Fig. 2.— Horizontally-averaged magnetic pressure versus height and time. The grey scale is linear from zero (white) to 3×10^6 dyn cm $^{-2}$ (black).

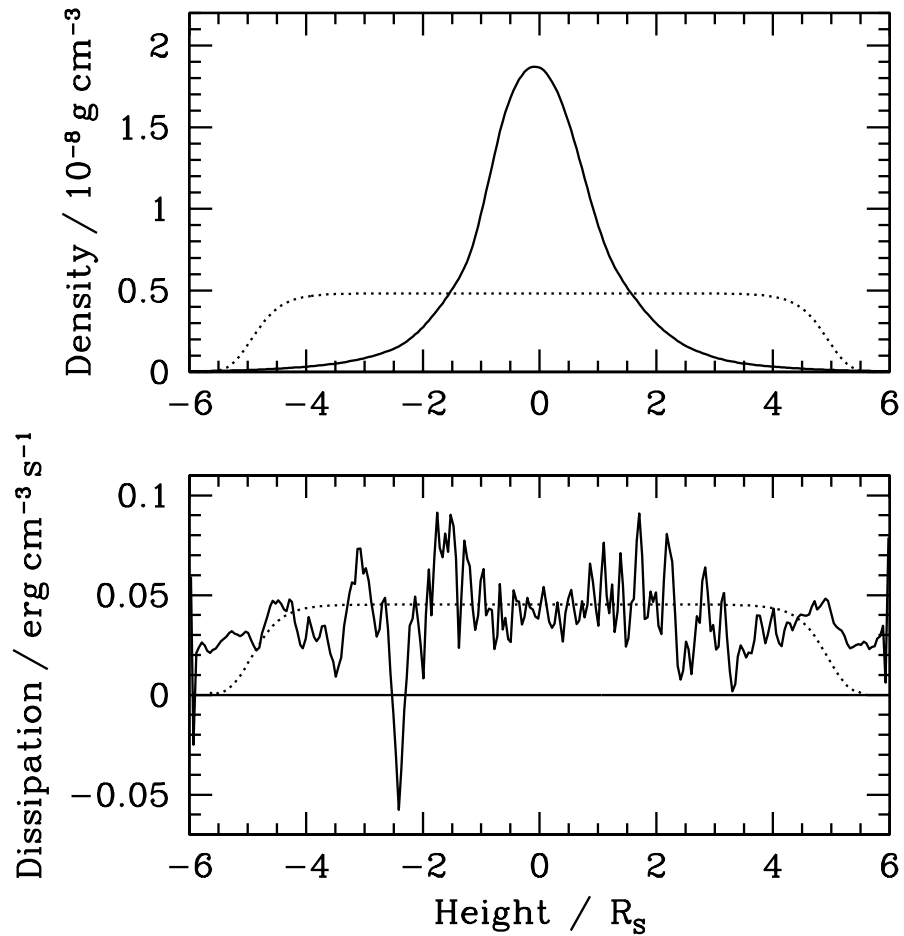


Fig. 3.— Simulation results (solid) compared with the Shakura-Sunyaev model (dotted) having the same surface density and radiation flux. Density is shown at top, total dissipation below. The simulation results are averaged horizontally, and over time from 15 to 45 orbits.